Supporting Information

Rapid, in situ Synthesis of Ultra-Small Silicon Particles for Boosted Lithium Storage Capability through Ultrafast Joule Heating

Shigang Liu [a,b,1], Bowen Liu [b,c,1], Ming Liu [b,c], Junjie Xiong [b,c], Yang Gao [b,c,*], Bin Wang [b,c,*], Yingcheng Hu [a,*]

[a] *Key Laboratory of Bio-based Material Science and Technology of Ministry of Education, Engineering Research Center of Advanced Wooden Materials of Ministry of Education, College of Material Science and Engineering, Northeast Forestry University, Harbin 150040, China*

[b] *CAS Key Laboratory of Nanosystem and Hierarchical Fabrication, National Center for Nanoscience and Technology, Beijing 100190, China*

[c] *University of Chinese Academy of Sciences, Beijing 100049, China*

[*] Corresponding authors.

E-mail addresses: yingchenghu@nefu.edu.cn (Y. Hu), gaoyang@nanoctr.cn (Y. Gao), wangb@nanoctr.cn (B. Wang).

[1] These authors contributed equally to this work.

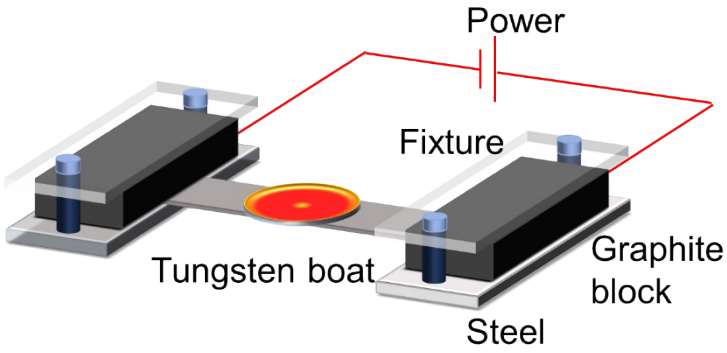

Figure S1. Schematic diagram illustrating the process of us-Si/C preparation utilizing a FJH apparatus.

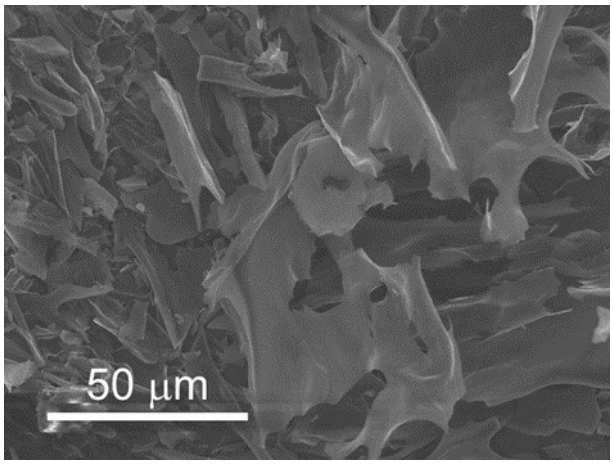

Figure S2. SEM image of CNCs, indicating that CNCs are freeze-dried and self-assembled into large scale nanosheet structures.

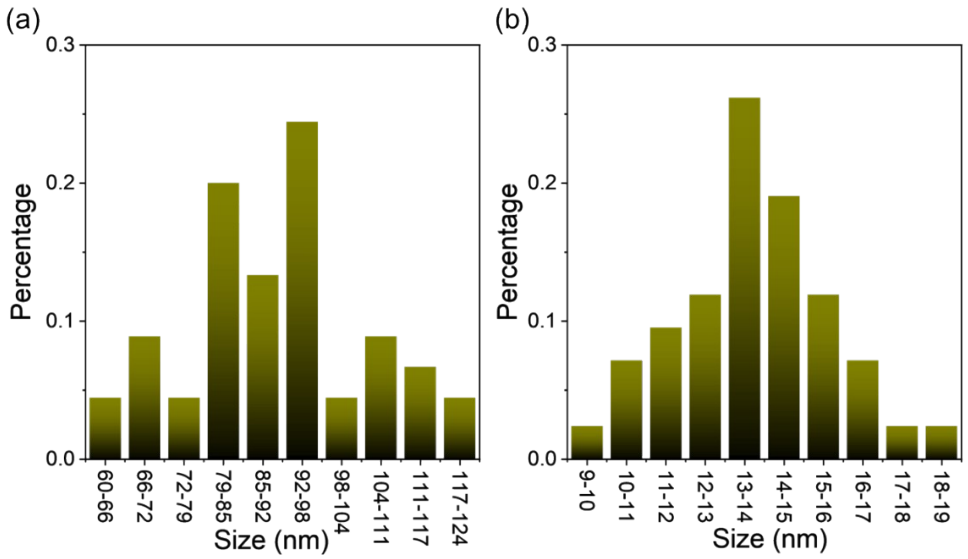

Figure S3. The size distribution of SiNPs in (a) Si/C and (b) us-Si/C.

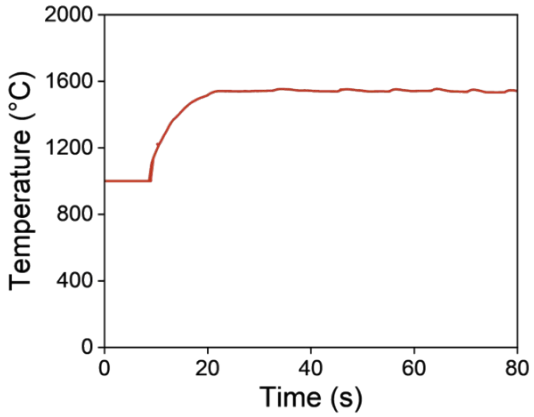

Figure S4. Temperature profile and stabilization trend of the FJH process.

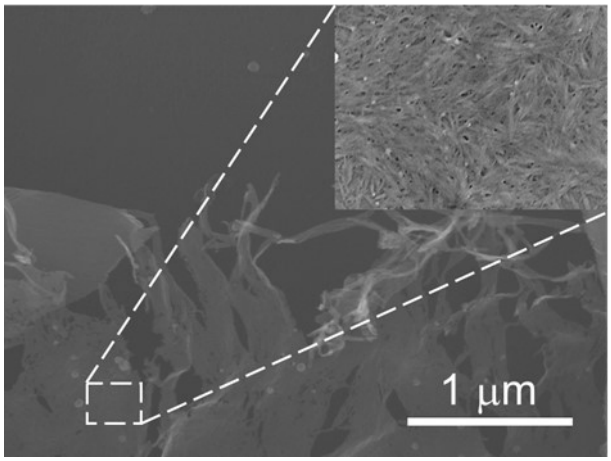

Figure S5. SEM image of carbon nanosheets derived from assembled CNCs.

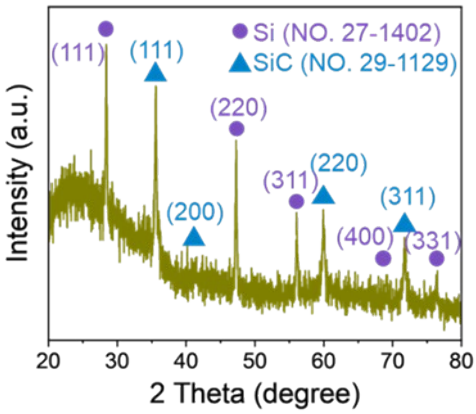

Figure S6. XRD pattern of the Si/C sample after continuous heating at 1700 °C for 50 s.

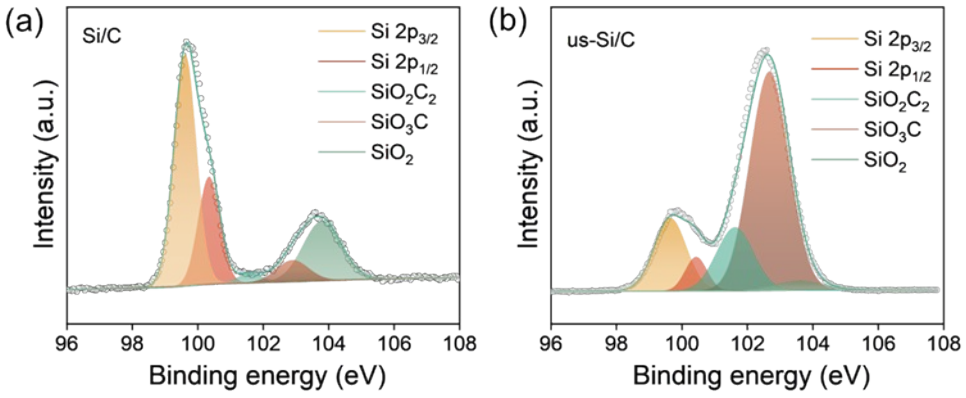

Figure S7. The high-resolution Si 2p XPS spectra of (a) Si/C and (b) us-Si/C.

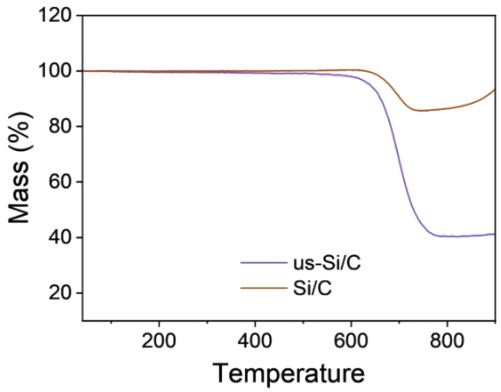

Figure S8. TG analysis of Si/C and us-Si/C under air condition.

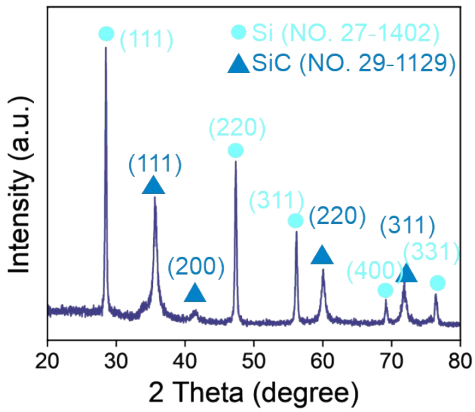

Figure S9. XRD pattern of the Si/C sample after being heated to 1200 °C for 3 h during CVD.

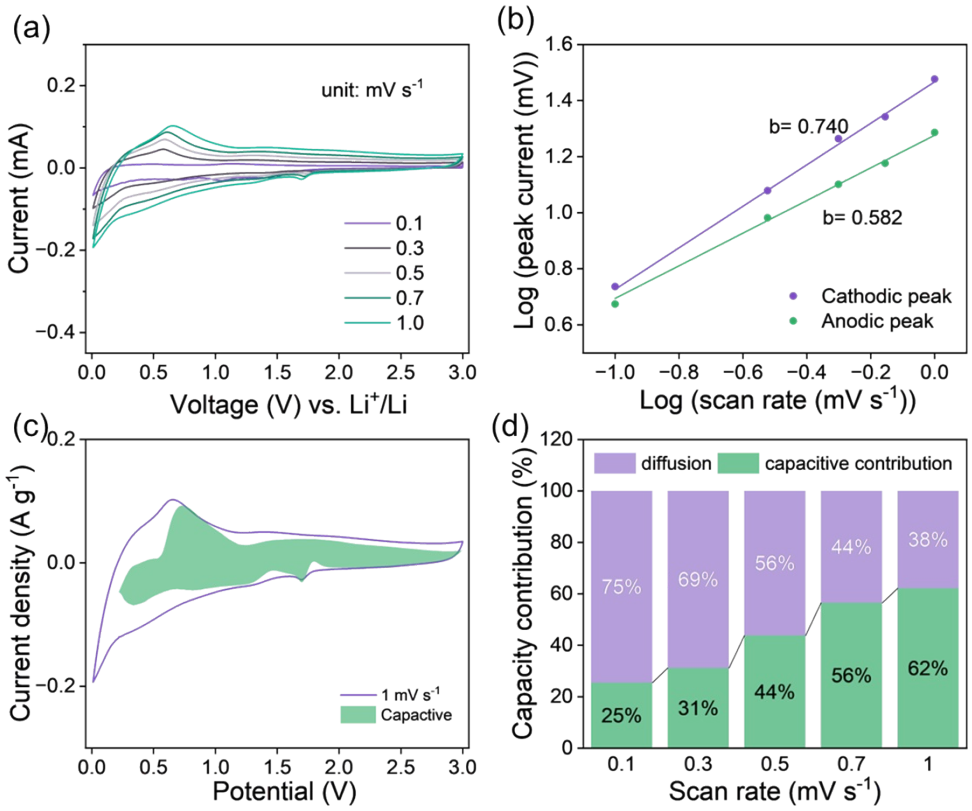

Figure S10. (a) CV curves of Si/C at different scan rates. (b) Logarithm of peak current vs. logarithm of scan rate. (c) Capacitive contribution to charge storage collected at 1.0 mV s^{-1}. (d) Capacitive and diffusion-controlled contribution to the total capacity at scan rates from 0.1 to 1.0 mV s^{-1}.

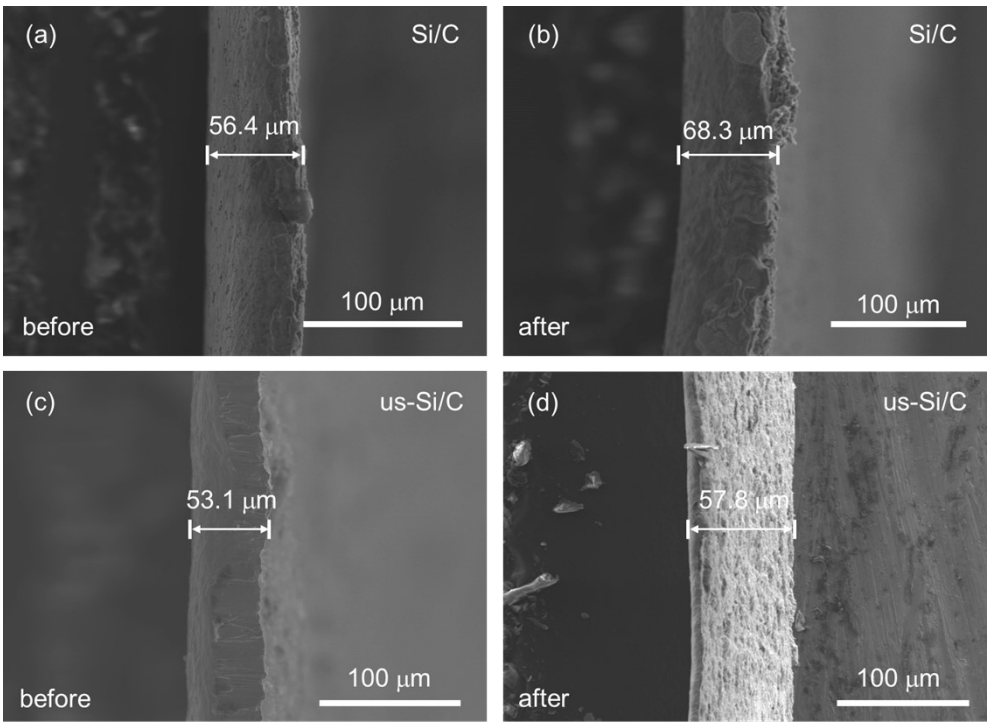

Figure S11. Cross-sectional morphology of (a) Si/C and (c) us-Si/C electrodes at the initial state. Cross-sectional morphology of (b) Si/C and (d) us-Si/C electrodes after 200 cycles.

Table S1. Electrochemical lithium storage properties of various Si/rGO composite electrode materials reported.

Materials	Si particle size	Voltage window (V)	Current density (mA g^{-1})	Capacity (mAh g^{-1})/cycle numbers	Ref.
Si/graphite	0.5 μm	0.01-1.5	1 mA cm^{-2}	0.909 mAh cm^{-2}/50	[1]
Nano-Si/graphite/carbon composite	100 nm	0.01-1.5	100	700/50	[2]
G/Si NP pellet	60 nm	0.01-1.5	0.5 C	3 mAh cm^{-2}/50	[3]
Si/rGO core-shell	12 μm	0.01-1	1000	1258/300	[4]
Mesoporous Si/C	50 nm	0.01-2	100	617/100	[5]
Si/DDAC/N-GNS	80 nm	0.01-1	2000	1168/100	[6]
3D Si/G	50 nm	0.1-1	200	1909/100	[7]
Porous yin-yang hybrid	200 nm	0.01-1.5	3000	800/600	[8]
Spherical Si/G	2.5 μm	0.01-2	1000	722/50	[9]
Si/G/C nanofibers	200 nm	0.1-1.5	3000	900/200	[10]
Si/G-bubble film	50 nm	0.01-1	100	998/1000	[11]
G/Si nanowires array	50 nm	0.01-1.5	2000	684/1000	[12]
Walnut Si@Gra@Pc	125 nm	0.01-1	300	450/1000	[13]
Alternating rGO/Si/ rGO	85 nm	0.01-1	1500	1849/200	[14]
Freestanding rGO/Si film	~500 nm	0.01-1.25	1000	713/200	[15]
Porous 3D G/Si/G sandwich	~7 nm	0.01-1	600	360/194	[16]
This work	~15 nm	0.01-1	2000	918/1000	

Reference

[1] S.S. Hwang, C.G. Cho, H. Kim, *Electrochim. Acta,* 55 (2010) 3236-3239.

[2] L. Takacs, *Prog. Mater. Sci.,* 47 (2002) 355-414.

[3] I.H. Son, J. Hwan Park, S. Kwon, et al., *Nat. Commun.,* 6 (2015) 7393.

[4] W. Zhai, Q. Ai, L. Chen, et al., *Nano Res.,* 10 (2017) 4274-4283.

[5] Z. Xiao, N. Xia, L. Song, et al., *Ionics,* 26 (2020) 589-599.

[6] R. Ruffo, S.S. Hong, C.K. Chan, et al., *J. Phys. Chem. C,* 113 (2009) 11390-11398.

[7] M.-S. Wang, G.-L. Wang, S. Wang, et al., *Chem. Eng. J.,* 356 (2019) 895-903.

[8] Y. Jin, Y. Tan, X. Hu, et al., *ACS Appl. Mater. Interfaces,* 9 (2017) 15388-15393.

[9] M. Su, S. Liu, L. Tao, et al., *J. Electroanal. Chem.,* 844 (2019) 86-90.

[10] L. Fei, B.P. Williams, S.H. Yoo, et al., *ACS Appl. Mater. Interfaces,* 8 (2016) 5243-5250.

[11] Y. Shi, Z. Wu, L. Du, et al., *J. Mater. Sci. Mater. Electron.,* 29 (2018) 4526-4532.

[12] F. Miao, R. Miao, W. Wu, et al., *Mater. Lett.,* 228 (2018) 262-265.

[13] X. Ding, W. Yao, J. Zhu, et al., *BioMed Res. Int,* 2020 (2020) 6173618.

[14] B. Deng, R. Xu, X. Wang, et al., *Energy Stor. Mater.,* 22 (2019) 450-460.

[15] X. Cai, W. Liu, Z. Zhao, et al., *ACS Appl. Mater. Interfaces,* 11 (2019) 3897-3908.

[16] Z. Feng, C. Huang, A. Fu, et al., *Thin Solid Films,* 693 (2020) 137702.